

## The Fascinating Noncentrosymmetric Copper(II) Phosphates Synthesized via CsCl Salt-Inclusion

Qun Huang and Shiou-Jyh Hwu\*

Department of Chemistry, Clemson University, Clemson, South Carolina 29634-0973

Received September 26, 2002

Two new noncentrosymmetric (NCS) solids were isolated via high-temperature, salt-inclusion reactions,  $\text{Cs}_2\text{Cu}_7(\text{P}_2\text{O}_7)_4 \cdot 6\text{CsCl}$  (**1**, CU-9) and  $\text{Cs}_2\text{Cu}_5(\text{P}_2\text{O}_7)_3 \cdot 3\text{CsCl}$  (**2**, CU-11). These copper(II) phosphates exhibit novel open-framework structures conceptually templated by extended Cs–Cl salt. The latter resides cooperatively in the channels upon the formation of the NCS Cu–P–O frameworks, leading to the formation of fascinating salt lattices centered by the NaCl-type core. These new discoveries are significant for they may give rise to a new route for the templated synthesis of NCS solids. We are to show here the structural correlation of the newly discovered hybrid solids, and the role of the chlorine atoms in the “intergrowth” of covalent/ionic sublattices.

Porous materials that possess noncentrosymmetric (NCS) structures have enticed research efforts in materials design for their petitions in nonlinear applications and chiral synthesis.<sup>1</sup> NCS open-framework solids developed thus far have been primarily organic–inorganic composites, which enable the integration of organic based chiral templates. Our recent exploration of salt-inclusion reactions has resulted in a fascinating class of composite (hybrid) solids that are composed of mixed ionic and covalent sublattices.<sup>2</sup> In light of the prior synthesis of  $\text{CuPO}_4 \cdot \text{BaCl}_2$ ,<sup>2c</sup> whose structure

contains helical chains of alternating corner- and edge-shared  $\text{CuO}_4$  and  $\text{PO}_4$  units, we have continued the investigation of NCS open-framework solids via salt-inclusion reactions. Herein, we report two fascinating NCS open-frameworks that are templated by extended inorganic Cs–Cl salt, that is,  $\text{Cs}_2\text{Cu}_7(\text{P}_2\text{O}_7)_4 \cdot 6\text{CsCl}$  (**1**) and  $\text{Cs}_2\text{Cu}_5(\text{P}_2\text{O}_7)_3 \cdot 3\text{CsCl}$  (**2**).

- (2) (a) Hwu, S.-J.; Ulutagay-Kartin, M.; Clayhold, J. A.; Mackay, R.; Wardojo, T. A.; O'Connor, C. J.; Krawiec, M. *J. Am. Chem. Soc.* **2002**, *124*, 12404–12405. (b) Huang, Q.; Hwu, S.-J.; Mo, X. *Angew. Chem., Int. Ed.* **2001**, *40*, 1690–1693. (c) Huang, Q.; Ulutagay, M.; Michener, P. A.; Hwu, S.-J. *J. Am. Chem. Soc.* **1999**, *121*, 10323–10326. (d) Ulutagay, M.; Shimek, G. L.; Hwu, S.-J.; Taye, H. *Inorg. Chem.* **1998**, *37*, 1507–1512. (e) Etheredge, K. M. S.; Hwu, S.-J. *Inorg. Chem.* **1995**, *34*, 3123–3125.
- (3) Crystals of **1** were grown by employing reactive CsCl salt in a fused silica ampule under vacuum.  $\text{CuO}$  (7.0 mmol),  $\text{P}_2\text{O}_5$  (4.0 mmol), and CsCl (24.0 mmol) were mixed and ground in a nitrogen-filled drybox. The reaction mixture was heated to 700 °C and isothermed for 48 h, followed by slow cooling to 300 °C at 0.1 °C/min and then furnace cooling to room temperature. Yield ca. 80%, estimated by the intensity of PXRD patterns, was obtained. Crystals of **2** were grown by employing reactive CsCl salt in an open quartz container. After the structure determination of **1**, stoichiometric mixtures of  $\text{CsOH} \cdot \text{H}_2\text{O}$  (2.0 mmol),  $\text{Cu}(\text{OH})_2$  (7.0 mmol),  $(\text{NH}_4)_2\text{HPO}_4$  (8.0 mmol), and CsCl (6.0 mmol) were ground in air. The mixture was heated to 650 °C and isothermed for 72 h, followed by slow cooling to 25 °C at 0.1 °C/min. Yield ca. 90% was obtained.
- (4) Crystal data of **1**: light greenish column crystal (0.25 × 0.01 × 0.02 mm<sup>3</sup>),  $M_r = 2416.52$ , orthorhombic  $P2_12_12_1$  (No. 19) with  $a = 9.942$ –(1) Å,  $b = 13.810$ (2) Å,  $c = 30.703$ (4) Å,  $V = 4215.6$ (9) Å<sup>3</sup>,  $Z = 4$ ,  $\rho_{\text{calcd}} = 3.807 \text{ g cm}^{-3}$ . Data collection: Mo K $\alpha$  ( $\lambda = 0.71073$  Å) radiation,  $T = 293$ (2)K, 39306 measured with 10017 unique reflections, of which 9210 ( $I > 2.0\sigma(I)$ ) were used for the structure solution with the SHELXTL-Plus software package. The structure was solved by direct methods using the SHELXS-86 program and refined on  $|F|^2$  by least-squares, full-matrix techniques. Final  $R/R_w = 0.060/0.099$ , GOF = 1.15 for 375 parameters. The final Fourier difference synthesis showed minimum and maximum peaks of  $-1.77$  and  $+1.53 \text{ e/Å}^3$ . Crystal data of **2**: light greenish column crystal (0.20 × 0.05 × 0.02 mm<sup>3</sup>),  $M_r = 1610.42$ , orthorhombic  $Pna2_1$  (No. 33), with  $a = 13.9425$ –(3) Å,  $b = 20.429$ (1) Å,  $c = 9.8366$ (5) Å,  $V = 2801.7$ (2) Å<sup>3</sup>,  $Z = 4$ ,  $\rho_{\text{calcd}} = 3.818 \text{ g cm}^{-3}$ . Data collection: Mo K $\alpha$  ( $\lambda = 0.71073$  Å) radiation,  $T = 293$ (2) K, 19826 measured with 4272 unique reflections, of which 4263 ( $I > 2.0\sigma(I)$ ) were used for the structure solution. Final  $R/R_w$  ( $|F|^2$ ) = 0.059/0.133, GOF = 1.30 for 256 parameters. The final Fourier difference synthesis showed minimum and maximum peaks of  $-1.13$  and  $+1.78 \text{ e/Å}^3$ . (a) TEXSAN: Single-Crystal Structure Analysis Software, Version 1.6b; Molecular Structure Corp.: The Woodlands, TX 1993. (b) Cromer, D. T.; Waber, J. T. Scattering Factors for Non-hydrogen Atoms. In *International Tables for X-ray Crystallography*; Kynoch Press: Birmingham, England, 1974; Vol. IV, Table 2.2A, pp 71–98. (c) Sheldrick, G. M. In *Crystallographic Computing 3*; Sheldrick, G. M., Krüger, C., Goddard, R., Eds.; Oxford University Press: London/New York, 1985; pp 175–189. (d) G. M. Sheldrick, SHELXS-93; University of Göttingen: Göttingen, Germany, 1993.

\* Corresponding author. E-mail: shwu@clemson.edu.

- (1) (a) Yu, J. H.; Wang, Y.; Shi, Z.; Xu, R. R. *Chin. J. Inorg. Chem.* **2002**, *18*, 51–55. (b) Schäfer, G.; Carrillo-Cabrera, W.; Leoni, S.; Borrmann, H.; Kniep, R. Z. *Anorg. Allg. Chem.* **2002**, *628*, 67–76. (c) Guo, Y.; Shi, Z.; Yu, J.; Wang, J.; Liu, Y.; Bai, N.; Pang, W. *Chem. Mater.* **2001**, *13*, 203–207. (d) Lin, C. H.; Wang, S. L. *Inorg. Chem.* **2001**, *40*, 2918–2921. (e) Kepert, C. J.; Prior, T. J.; Rosseinsky, M. J. *J. Am. Chem. Soc.* **2000**, *122*, 5158–5168. (f) Giraldo, O.; Marquez, M.; Brock, S. L.; Suib, S. L.; Hillhouse, H.; Tsapatsis, M. *J. Am. Chem. Soc.* **2000**, *122*, 12158–12163. (g) Yan, W. F.; Yu, J. H.; Shi, Z.; Xu, R. R. *Chem. Commun.* **2000**, 1431–1432. (h) Zheng, L. M.; Whitfield, T.; Wang, X. Q.; Jacobson, A. J. *Angew. Chem., Int. Ed.* **2000**, *39*, 4528–4531. (i) Bein, T. *Curr. Opin. Solid State Mater. Sci.* **1999**, *4*, 85–96. (j) Neeraj, S.; Natarajan, S.; Rao, C. N. R. *Chem. Commun.* **1999**, 165–166. (k) Gier, T. E.; Bu, X. H.; Feng, P. Y.; Stucky, G. D. *Nature* **1998**, *395*, 154–157. (l) Ayyappan, S.; Bu, X.; Cheetham, A. K.; Rao, C. N. R. *Chem. Mater.* **1998**, *10*, 3308–3310. (m) Stalder, S. M.; Wilkinson, A. P. *Chem. Mater.* **1997**, *9*, 2168–2173. (n) Gray, M. J.; Jasper, J. D.; Wilkinson, A. P.; Hanson, J. C. *Chem. Mater.* **1997**, *9*, 976–980. (o) Feng, P. Y.; Bu, X. H.; Tolbert, S. H.; Stucky, G. D. *J. Am. Chem. Soc.* **1997**, *119*, 2497–2504.

## COMMUNICATION

Compounds **1** and **2** were synthesized in the molten CsCl medium (mp 645 °C).<sup>3</sup> Single-crystal structures were determined by the X-ray diffraction methods.<sup>4</sup> Compound **1**, which is chiral, crystallizes in one of the 11 NCS nonpolar crystal classes,  $222 (D_2)$ , and **2**, which is nonchiral, in one of the 10 NCS polar crystal classes,  $mm2 (C_{2v})$ .<sup>5</sup> Second-harmonic generation measurements using a powder method previously described<sup>6</sup> gave no sign of frequency doubling, which is mostly due to the lack of polarizable elements in the structures. The chemical contents were confirmed by qualitative EDAX analysis and stoichiometric synthesis.

The title compounds (designated as CU-9 and CU-11, respectively) are new additions to the CU family, which exhibits a hybrid framework of mixed covalent and ionic sublattices. The covalent sublattices characteristically form pseudo-one-dimensional channels where the extended salt resides. In the most studied CU–CuPO series, the Cu–P–O sublattices consist of negatively charged  $\text{Cu}_{2n-1}(\text{P}_2\text{O}_7)_n^{2-}$  open-frameworks, for example,  $\text{Cu}_3(\text{P}_2\text{O}_7)_2^{2-}$  ( $n = 2$ ) for CU-2 and 4.<sup>2b,c</sup> The newly discovered Cu–P–O frameworks are  $\text{Cu}_7(\text{P}_2\text{O}_7)_4^{2-}$  ( $n = 4$ ) and  $\text{Cu}_5(\text{P}_2\text{O}_7)_3^{2-}$  ( $n = 3$ ) and, as shown in Figure 1, display single-size channels with parallelogram (20-ring) and heart-shaped (16-ring) windows, respectively.

It is intriguing to see the additional role of salt lattice in facilitating the formation of NCS structures. Figure 2 depicts the extended Cs–Cl structure found in **1** (left), which is centered by a column of the NaCl-type  $[\text{Cs}_4\text{Cl}_4]_\infty$  core. It is worth noting that the extended salt lattice of **2** (right) literally adopts one-half of the NaCl-type core observed in **1**, thus the formation of smaller pore structure. In addition, the ordering of copper cations in the Cu–P–O frameworks is dictated by the relative positions of the  $\text{Cl}^-$  anions in extended salt lattice (see later).

All the chloride anions adopt six-coordination to either  $4\text{Cs}^+/2\text{Cu}^{2+}$  or  $5\text{Cs}^+/1\text{Cu}^{2+}$  cations in a distorted octahedral geometry, a common coordination adopted by metal chlorides. The bridging copper atoms, Cu(4,5) in **1** and Cu(5) in **2**, adopt the shortest Cu–Cl distances in the  $\text{CuO}_2\text{Cl}_2$  unit, for example, 2.21–2.29 Å, which are shorter than 2.38 Å, the sum of Shannon crystal radii of tetrahedrally coordinated  $\text{Cu}^{2+}$  (0.71 Å) and  $\text{Cl}^-$  (1.67 Å).<sup>7</sup> The terminal coppers, Cu(1,2,3,6,7) in **1** and Cu(1,2,3,4) in **2**, give rise to long Cu–Cl distances, for example, 2.63–3.32 Å, much longer than 2.54 Å of the expected distance of an ideal octahedral geometry. The corresponding chlorine atoms occupy the apical positions of the  $\text{Cu}^{2+}$ -centered square pyramidal  $\text{CuO}_4\text{Cl}$  and octahedral  $\text{CuO}_4\text{Cl}_2$  units, similarly observed in the chlorooxocuprates.<sup>8</sup> The tetragonal elongation along the Cu–Cl bonds is attributed to the  $d^9 \text{Cu}^{2+}$  Jahn–Teller distortion

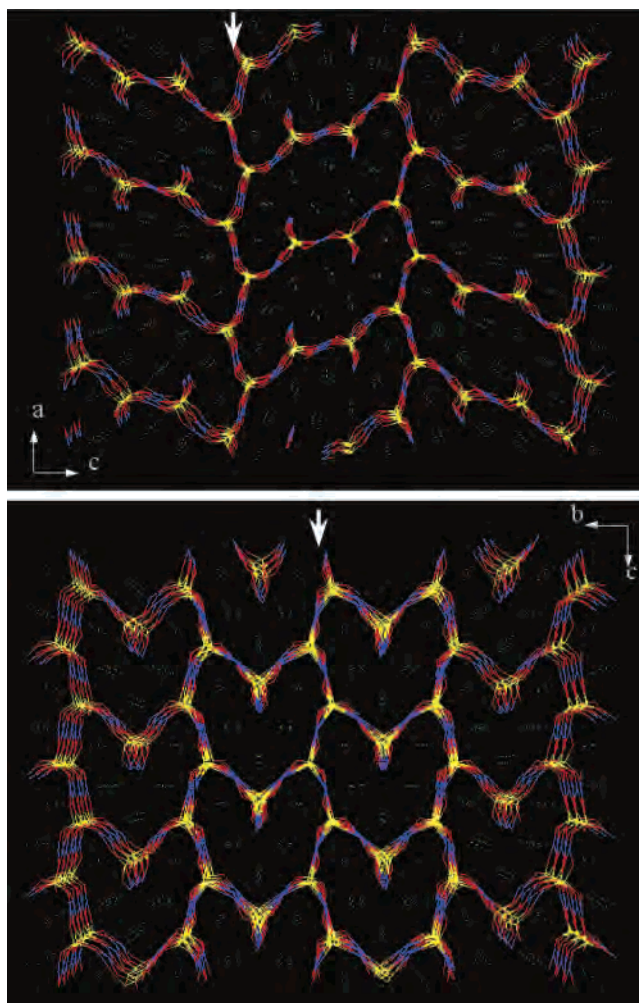


**Figure 1.** Perspective views showing the structures of  $\text{Cs}_2\text{Cu}_7(\text{P}_2\text{O}_7)_4 \cdot 6\text{CsCl}$  (top) and  $\text{Cs}_2\text{Cu}_5(\text{P}_2\text{O}_7)_3 \cdot 3\text{CsCl}$  (bottom). The Cu–P–O frameworks are outlined by Cu-centered bonds drawn in blue, P in yellow, and O in red, while the nonbonded Cl is drawn in green and Cs in white. Arrows indicate the direction of the  $2_1$ -screw axis (see text).

and the structural incommensuration due to the intergrowth of covalent and ionic sublattices.<sup>9</sup>

It is interesting to observe that, despite the different window geometry, **1** and **2** share a common Cu–P–O network structure along the (002) and (020) planes, respectively, where the  $2_1$ -screw axes lie (see Figure 1). The network structure, as shown in Figure 3, consists of alternating  $\text{CuO}_4$  square-planar and  $\text{P}_2\text{O}_7$  pyrophosphate units. Each  $\text{CuO}_4$  shares oxygen atoms with three  $\text{P}_2\text{O}_7$ , one bridges via two *cis* oxygen atoms and two others each link via one oxygen. This gives rise to the  $1\text{CuO}_4/3\text{P}_2\text{O}_7$  connectivity across the networks. In contrast, the open-frameworks of the previously identified CU-2 and CU-4, exhibiting alternating 18-/8-ring windows, consist of a mixed  $1\text{CuO}_4/2\text{P}_2\text{O}_7$  (in a doubly bridged *trans* fashion) and  $1\text{CuO}_4/4\text{P}_2\text{O}_7$  connectivity.<sup>3b,c</sup> The wide range framework variation, once again, exemplifies the versatility of transition metal phosphate structures, as similarly seen in a vast number of open-framework aluminosilicates and aluminophosphates.<sup>10</sup>

(5) (a) Halasyamani, P. S.; Poeppelmeier, K. R. *Chem. Mater.* **1998**, *10*, 2753–2769. (b) NCS space groups were chosen on the basis of comparison using Friedel pairs. The absolute configuration was determined by the Flack factor; a value of zero was given in the final refinement indicating a correct configuration.

(6) Porter, Y.; Ok, K. M.; Bhuvanesh, N. S. P.; Halasyamani, P. S. *Chem. Mater.* **2001**, *13*, 1910–1915.

(7) Shannon, R. D. *Acta Crystallogr., Sect. A* **1976**, *32*, 751–767.

(8) Müller-Buschbaum, H. *Angew. Chem., Int. Ed. Engl.* **1977**, *16*, 674–687.

(9) Kunz, M.; Brown, I. D. *J. Solid State Chem.* **1995**, *115*, 395–406.

(10) Huang, Q.; Hwu, S.-J. *Chem. Commun.* **1999**, 2343–2344 and references therein.

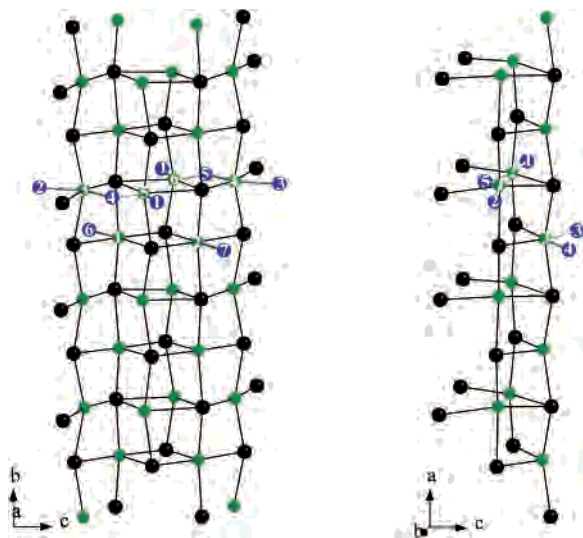


**Figure 2.** Extended salt sublattices of **1** (left) and **2** (right) showing the connectivity with copper cations. Each chlorine coordinates to six cations; for clarity, only one asymmetric unit of Cu and Cl is labeled. The bridging copper atoms form the shortest Cu–Cl bonds (see text).

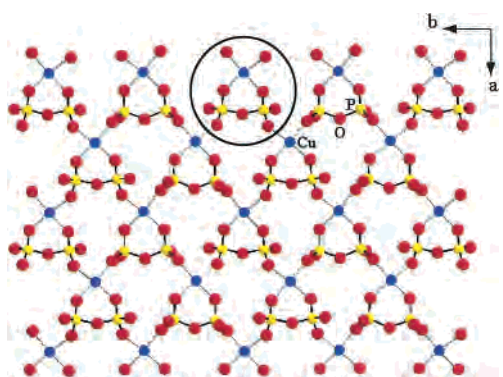


**Figure 3.** Partial structure of **1** showing the Cu–P–O network along the (002) plane. The (020) plane of **2** adopts exactly the same connectivity. The building block (circled) of the network structure consists of one  $\text{CuO}_4$  and a  $\text{P}_2\text{O}_7$  bridging unit (see text).

The network consists of corner-shared  $\text{CuO}_4/\text{P}_2\text{O}_7$  building blocks (as shown by the circled unit in Figure 3), and the orientation of these units determines the polarity of extended lattices. The representative network structure shown in Figure 3 reveals a polar axis along *a* because all the  $\text{P}_2\text{O}_7$  units lay on one side of the bridged  $\text{CuO}_4$ . In **1**, the polar axes of neighboring networks point in opposite directions leading to the cancellation of polarity and, subsequently, the formation of nonpolar lattice. In **2**, however, the polar axes of neighboring networks point in one direction, therefore, the formation of polar lattice.

Compounds **1** and **2** share additional structural features, whereas the parallelogram-shaped window can be considered as the result of pore condensation of two inverted heart-shaped windows. This can be realized by a close comparison of two framework structures that link parallel slabs of the Cu–P–O networks. As shown in Figure 4, the center  $\text{P}_2\text{O}_7$  unit in **2** (right) shares its oxygen atoms along *b* with two square-planar  $\text{CuO}_4$  groups in a *trans* fashion keeping the  $1\text{CuO}_4/3\text{P}_2\text{O}_7$  configuration. It shares the opposite oxygen atoms each along *a* with two tetrahedral  $\text{CuO}_2\text{Cl}_2$  units to

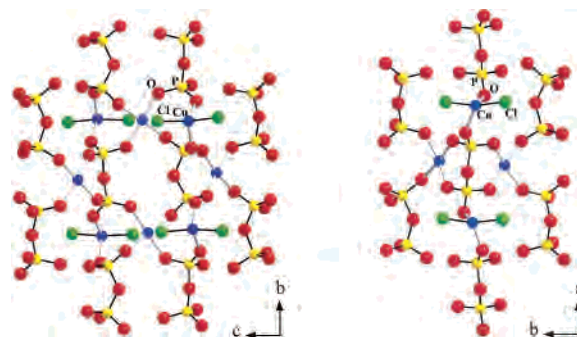


**Figure 4.** Framework structures of **1** (left) and **2** (right) showing the connectivity between parallel network slabs (represented by the outer columns of  $\text{P}_2\text{O}_7$  units) shown in Figure 3.

propagate into a linear chain. The  $\text{CuO}_2\text{Cl}_2$  units are realized as nonframework units tipping into the channels (Figure 1). Compound **1** (Figure 4, left), otherwise, consists of two such linear chains interlinked by additional square-planar  $\text{CuO}_4$  units, which adopt the  $1\text{CuO}_4/4\text{P}_2\text{O}_7$  configuration.

The anionic frameworks of **1** and **2** can be formulated as  $[\text{Cu}_{2/1}\text{Cu}_{10/2}(\text{P}_2\text{O}_7)_{4/2}(\text{P}_2\text{O}_7)_{6/3}]^{2-}$  and  $[\text{Cu}_{1/1}\text{Cu}_{8/2}(\text{P}_2\text{O}_7)_{2/2}(\text{P}_2\text{O}_7)_{6/3}]^{2-}$ , respectively. The former consists of 2 non-framework and 10 framework Cu, four  $\text{P}_2\text{O}_7$  groups that are shared by 2 window units, and 6 more  $\text{P}_2\text{O}_7$  groups shared at the joint of 3 neighboring window units (Figure 1). The  $10\text{CuO}_4/(4+6)\text{PO}_4$  polyhedra sum up to the 20-ring (with respect to the total number of  $\text{Cu}^{2+}$  and  $\text{P}^{5+}$ ) window. Likewise, the formula of **2** reflects one nonframework Cu and the 16-ring ( $8\text{CuO}_4/(2+6)\text{PO}_4$ ) structure.

As a final remark, the structural principles discussed here lead to an outline of the fascinating NCS open-frameworks and extended salt lattices. Several recent reports also have demonstrated the utility of inorganic salt for the formation of novel frameworks.<sup>11</sup> The current discoveries reaffirm the implications to the synthesis of noncentrosymmetric solids via salt-inclusion.

**Acknowledgment.** Financial support for this research (Grants DMR-0077321 and EPS-9977797) and the purchase of the single crystal X-ray diffractometer (Grant CHE-9808165) from the National Science Foundation is gratefully acknowledged. We also thank Prof. P. Shiv Halasyamani for the second-harmonic generation measurements.

**Supporting Information Available:** Detailed description of bulk synthesis, X-ray crystallographic files, in CIF format, including tables of crystallographic details, atomic coordinates, anisotropic thermal parameters, and interatomic distances and angles. This material is available free of charge via the Internet at <http://pubs.acs.org>.

IC026060I

- (11) (a)  $\text{Cs}_2\text{Bi}_{10}\text{Ca}_6\text{Cl}_{12}\text{O}_{16}$ : Harris, K. D. M.; Ueda, W.; Thomas, J. M.; Smith, G. W. *Angew. Chem., Int. Ed. Engl.* **1988**, *27*, 1364–1365. (b)  $\text{AHg}_2\text{O}_2\text{Cl}_2$  (A = Sr, Ba): Harrison, W. T. A.; Liu, L.; Jacobson, A. J. *Angew. Chem., Int. Ed. Engl.* **1996**, *35*, 625–627. Harrison, W. T. A.; Liu, L.; Jacobson, A. J.; Vogt, T. *Inorg. Chem.* **1998**, *37*, 834–835. (c) Salt-containing cadmium oxalates: Vaidhyanathan, R.; Natarajan, S.; Rao, C. N. R. *Chem. Mater.* **2001**, *13*, 3524–3533. Vaidhyanathan, R.; Neeraj, S.; Prasad, P. A.; Natarajan, S.; Rao, C. N. R. *Angew. Chem., Int. Ed.* **2000**, *39*, 3470–3473.